This is an open access article published under an ACS AuthorChoice License, which permits copying and redistribution of the article or any adaptations for non-commercial purposes.

BIOCHEMISTRY
including biophysical chemistry & molecular biology

Article

pubs.acs.org/biochemistry

Role of the Coiled-Coil Structural Motif in Polyglutamine Aggregation

Bashkim Kokona, Zachary P. Rosenthal, and Robert Fairman*

Department of Biology, Haverford College, 370 Lancaster Avenue, Haverford, Pennsylvania 19041, United States

Supporting Information

ABSTRACT: Polyglutamine repeat motifs are known to induce protein aggregation in various neurodegenerative diseases, and flanking sequences can modulate this behavior. It has been proposed that the 17 N-terminal residues (Htt^{NT}) of the polyglutamine-containing huntingtin protein accelerate the kinetics of aggregation due to the formation of helix-rich oligomers through helix-pairing interactions. Several hypotheses that explain the role of helical interactions in modulating aggregation have been proposed. These include (1) an increase in the effective concentration of polyglutamine chains (proximity model), (2) the induction of helical structure within the polyglutamine domain itself (transformation model), and/or (3) interdomain interactions between the flanking sequence and the polyglutamine domain (domain cross-talk model). These hypotheses are tested by studying the kinetics of polyglutamine aggregation using a Q_{25} sequence fused to a well-defined heterotetrameric coiled-coil model system. Using a combined spectroscopic and dye binding approach, it is shown that stable coiled-coil formation strongly inhibits polyglutamine aggregation, suggesting that the proximity and transformation models are insufficient to explain the enhanced aggregation seen in Htt^{NT}–polyglutamine constructs. Consistent with other published work, our data support a model in which domain cross-talk prevents formation of a nonspecific aggregated collapsed polyglutamine state, which can act to inhibit conversion to a fibrillar state. Because our model system has a charged to nonpolar residue ratio much higher than that of the Htt^{NT} sequence, domain cross-talk is severely weakened, thus favoring the nonspecific aggregation pathway and significantly inhibiting aggregation through a fibrillar pathway.

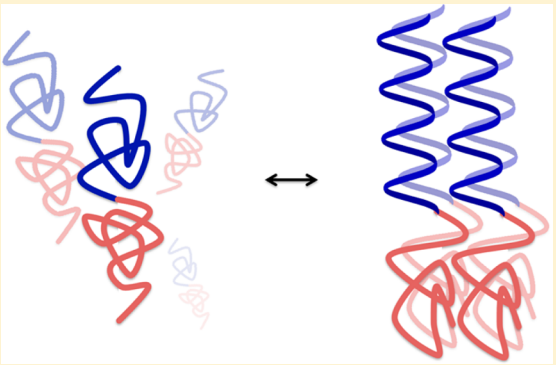

The molecular mechanism of aggregation of polyglutamine-containing proteins is of strong interest because of the role of such proteins in a variety of human diseases, including Huntington's disease and a group of spinocerebellar ataxias.[1] Like several other neurodegenerative diseases involving protein aggregation, such as Alzheimer's disease and Parkinson's disease, the underlying structural mechanism for such aggregation is thought to involve the formation of cross-β-sheet structures whose individual strands are open-ended in their hydrogen bonding potential.[2] Polyglutamine stretches with 35 or more glutamines are prone to aggregate through such a cross-β-sheet assembly process, most likely involving interdigitated glutamine side chains. This interdigitation fosters both nonpolar and hydrogen bonding interactions in what has been termed a steric zipper geometry,[3] a view that is supplanting the classic polar zipper model.[4]

Interestingly, several laboratories have now shown that sequences that are involved in cross-β-sheet fibrillization might proceed through a helical intermediate, involving helix-pairing interactions,[5−7] and models for this have recently been reviewed by Abedini and Raleigh.[8,9] Evidence of such intermediates in disease has been demonstrated for Aβ (Alzheimer's disease)[5] and IAPP,[6,10] among others. In the reviews by Abedini and Raleigh,[8,9] they summarize work that suggests that the helical conformation could mediate helix-pairing interactions, particularly if the sequences involved are rich in hydrophobic amino acids and at least partially amphipathic in their amino acid distribution. This helix-pairing effect (whether homogeneous or heterogeneous in its final aggregated state) would create a high effective concentration of aggregation-prone sequences that would then help to drive cross-β-sheet formation, thus leading to faster cross-β-sheet aggregation (herein termed the "proximity" model). Evidence of such helical interactions in the N-terminal (Htt^{NT}) polyglutamine-flanking sequence of the huntingtin protein[11−14] has also been used as support for the proximity model.[13,15]

More recently, it has become clear that flanking sequences containing helical domains, such as that described above for the huntingtin protein, play a significant role in the kinetics of assembly specifically in polyglutamine-containing proteins.[1,16] A sequence-mining survey by Kandel, Hendrickson, and others[17] was conducted, and they found that predicted coiled-coil sequences proximal to polyglutamine sequences are quite common and thus are strongly implicated in influencing polyglutamine aggregation potential. They pro-

Received: April 13, 2014
Revised: September 20, 2014
Published: October 13, 2014

 © 2014 American Chemical Society dx.doi.org/10.1021/bi500449a | *Biochemistry* 2014, 53, 6738−6746

Table 1. Peptide Sequences

$KKQ_{25}KK$:	KKQQQQQQQQQQQQQQQQQQQQQQQQQKK
Htt^{NT}:	MATLEKLMKAFESLKSF
$Htt^{NT}Q_{25}KK$:	MATLEKLMKAFESLKSF QQQQQQQQQQQQQQQQQQQQQQQQQKK
Htt^{NT}-Ω-$Q_{25}KK$:	MATLEKLMKAFESLKSF GGSPGGS QQQQQQQQQQQQQQQQQQQQQQQQQKK
ecK:	MKKIKDKLEKIKSKLYKIKNELAKIKKL
ecE:	MKEIEDKLEEIESKLYEIENELAEIEKL
ecK$Q_{25}KK$:	MKKIKDKLEKIKSKLYKIKNELAKIKKL QQQQQQQQQQQQQQQQQQQQQQQQQKK
ecK-Ω-$Q_{25}KK$:	MKKIKDKLEKIKSKLYKIKNELAKIKKL GGSPGGS QQQQQQQQQQQQQQQQQQQQQQQQQKK

posed a model in which the helical conformation in coiled coils propagates through the polyglutamine sequence and acts as a critical intermediate in aggregation (herein termed the polyglutamine "transformation" model). As mentioned above, a 17-residue N-terminal domain (Htt^{NT}) in the huntingtin protein is known to greatly accelerate polyglutamine aggregation and is thought to do so through the formation of a nonspecific but self-limiting oligomerization process induced by helical interactions,[18] perhaps akin to the types of interactions seen in coiled coils, and may result in propagation through the polyglutamine domain. Both the proximity and transformation models are tested in the work presented here using model systems containing polyglutamine sequences with helical flanking domains.

More complex models that involve various direct interactions between flanking sequences and the polyglutamine domain have been proposed.[12,15,16,19−21] Such interactions may involve a variety of structural characteristics, most notably those involving the spectrum of collapsed states (including possible molten globule states) in either the flanking domains or the polyglutamine domain itself. These models are collectively termed "domain cross-talk" models, involving intrachain, interdomain contacts. Evidence of the role of such collapsed states in promoting protein fibrillization is not new[22] and has been explored again recently, focusing on chemical characteristics of flanking domains (such as polarity) that might influence such cross-talk. Furthermore, the lack of structural specificity in flanking domains likely also influences the inherent heterogeneity in oligomerization that is often present, and thus further modulates polyglutamine aggregation.[19−21,23]

In summary, the hypotheses that have been proposed to probe the mechanisms of how the helical motif modulates polyglutamine aggregation include (1) increasing the effective concentration of polyglutamine chains through helix-pairing interactions (proximity model), (2) helix propagation into the polyglutamine sequence as a catalyst of aggregation (transformation model), and (3) interactions between helix-rich domains and a polyglutamine sequence (domain cross-talk model). Biophysical features of the coiled coil would influence the aggregation mechanism in any of these proposed hypotheses and include factors such as structural stability and dynamics, as well as the degree and specificity of oligomerization. These competing hypotheses for the effects of putative coiled-coil domains on polyglutamine aggregation invite a deeper analysis of the structural role that the helical conformation might play in protein aggregation. If such helix-rich domains are confirmed as general effectors of the aggregation process, then affecting their assembly may provide additional opportunities for intervention in human polyglutamine diseases.

Our heterotetrameric coiled-coil system is applied here, involving the interaction of parallel helices that had been designed some time ago[24] to test various elements of these hypotheses and structural features. The nature of this system allows us to study the effects of both weakly associating (homotetrameric) and tightly associating (heterotetrameric) helices on polyglutamine aggregation. More structural details of this system are described below.

MATERIALS AND METHODS

Peptide Synthesis and Purification. Htt^{NT}, $Htt^{NT}Q_{25}KK$, ecK, and ecE peptides were synthesized on site using an Applied Biosystems 433A peptide synthesizer with Fmoc chemistry. $Htt^{NT}Q_{25}KK$ was purified as a mixture with an impurity containing a one-glutamine deletion. The problems with such impurities are well-known for polyglutamine-containing peptides. $KKQ_{25}KK$, Htt^{NT}-Ω-$Q_{25}KK$, ecK-Ω-$Q_{25}KK$, and ecK$Q_{25}KK$ peptides were purchased from the Yale University Keck Biotechnology Center (http://keck.med.yale.edu/) (Table 1).

Crude peptides were purified using reversed phase high-performance liquid chromatography (RP-HPLC) using a mobile phase of water and acetonitrile with 0.1% TFA on a Varian ProStar system equipped with a Varian Dynamax semipreparative C18 column. Htt^{NT}-Ω-$Q_{25}KK$ and $Htt^{NT}Q_{25}KK$ peptides were purified using a Vydac semi-preparative protein C4 column. Peptide identities were confirmed using MALDI-TOF mass spectrometry, yielding the following molecular masses (in daltons, reported as experimental, theoretical): $KKQ_{25}KK$ (3734.6, 3734.0), ecK$Q_{25}KK$ (6904.6, 6903.0), ecK-Ω-$Q_{25}KK$ (7425.1, 7425.5), Htt^{NT} (2016.3, 2016.4), $Htt^{NT}Q_{25}KK$ (5476.1, 5476.7 and 5345.0 representing a glutamine deletion), and Htt^{NT}-Ω-$Q_{25}KK$ (5933.5, 5933.5 and 5805.7 representing a glutamine deletion). Confirmation of the masses of the other peptides used in this study has been previously reported.[24]

Disaggregation Protocol. Peptides were disaggregated as follows. In a scintillation vial, 2−3 mg of lyophilized peptide was dissolved in a 1:1 HFIP/TFA mixture and solubilized overnight at room temperature (HFIP and TFA were obtained from Sigma-Aldrich). After solubilization, the solutions were dried under a constant stream of N_2 for 1 h, after which a film formed around the vial walls. Samples were then further dried under vacuum for ∼30 min. Dried samples were dissolved in a H_2O/0.1% TFA mixture and filtered through a 0.2 μm low protein binding filter (Pall HT Tuffryn Membrane) to remove

dx.doi.org/10.1021/bi500449a | Biochemistry 2014, 53, 6738−6746

larger scale aggregates. Samples were then transferred for centrifugation to a polycarbonate thick-wall tube and placed into SW 50.1 rotor adapters. The adapters were then placed onto an SW 50.1 rotor and prechilled at 4 °C. Samples were spun at 50000 rpm and 4 °C for 6 h. After centrifugation, the top ∼60% of the supernatant was removed. This procedure helped to remove smaller scale aggregates. An aliquot of 100 μL from the collected supernatant was used for concentration determination as well as in dynamic light scattering measurements for the final determination of residual aggregation. Protein stock solutions were again filtered through a 0.2 μm low protein binding filter. Stock concentrations were determined either by using a modified ninhydrin assay[25,26] or by measuring the tyrosine absorbance at 280 nm in 6 M GuHCl.[27] This disaggregation protocol was performed prior to each experiment and validated as a monomeric pool using dynamic light scattering.

Circular Dichroism Spectropolarimetry. Secondary structures of freshly disaggregated fibrils and of diluted mature fibrils were monitored using an Aviv 410 circular dichroism spectropolarimeter using a 1 mm path length quartz cuvette. Fibrils were diluted to a peptide concentration of 20 μM in 2.7 mM KCl, 136.9 mM NaCl, 1.5 mM potassium phosphate, and 8.9 mM sodium phosphate (pH 7.1) [PBS (pH 7.1)]. Scans were taken using a 1.5 nm bandwidth, ranging from 180 to 260 nm, using a step size of 0.5 nm, and an averaging time of 3 s. The reported spectra are buffer subtracted averages collected over three scans.

Fluorescence Spectroscopy. Dye binding experiments were performed using ThT, DCVJ, or ANS. Extinction coefficients for the dyes are 26620 M^{-1} cm^{-1} for ThT at 416 nm in ethanol,[28] 65900 M^{-1} cm^{-1} for DCVJ at 453 nm in a 50:50 ethanol/water mixture,[29] and 7800 M^{-1} cm^{-1} for ANS at 372 nm in 1 N NaOH.[24,30] Dye binding spectra were recorded using an F-7000 fluorescence spectrophotometer (Hitachi High-Technologies Corp.) with a 3 mm path length fluorescence cuvette. All samples were prepared in PBS (pH 7.1) unless stated otherwise. The kinetic data were fit to the following kinetic function:

$$y = \frac{A_1 - A_2}{1 + e^{(x - x_0)/dx}} + A_2$$

where A_1 and A_2 are the starting and ending absorbance signals, respectively, dx is the time constant for the transition, and x_0 represents the center of the transition along the x-axis.

Dynamic Light Scattering. All measurements were taken at 25 °C in PBS (pH 7.1). Data were collected using a DynaPro-MS/X dynamic light scattering instrument (Wyatt Technology, Santa Barbara, CA) equipped with an 825 nm laser set at 10% power. The temperature was controlled using a DynaPro temperature-controlled microsampler. Instrument operation, data collection, and analysis were managed using the Dynamics (version 6.0) software interface. Measurements were made using a 3 mm path length microcell cuvette to minimize sample volume. For each sample, a set of four independent measurements were made, with each measurement consisting of 30 runs each. Time-dependent fluctuations in the scattered light were analyzed using a second-order correlation function. Data were analyzed assuming a standard linear polysaccharide model, which most closely approximates the shape of ribbon fibrils.

Analytical Ultracentrifugation. Sedimentation velocity experiments were conducted in a Beckman Proteome Lab XL-A analytical ultracentrifuge equipped with an An60Ti rotor. Samples were run at 50000 rpm and 20 °C, collecting 150 scans per sample while using a time delay between scans of 300 s. Peptide concentrations ranged between 50 and 300 μM for ecK and Htt^{NT}. All samples were measured in PBS (pH 7.1) and 0.75 M NaCl. Temperature-dependent partial specific volumes (0.7982 mL g^{-1} for ecK and 0.7648 mL g^{-1} for Htt^{NT}), solution density (1.0311 g mL^{-1}), and viscosity (1.0807×10^{-2} Pa s) were calculated using SednTerp version 1.09.[31] Sedimentation velocity data were analyzed using DCDT+ version 2.4.0 (John Philo, Thousand Oaks, CA). Molecular masses for analyzed species were calculated from best fit $s_{20,w}$ and $D_{20,w}$ values using DCDT+.

RESULTS

This work takes advantage of the extensively studied polyglutamine peptide sequence, $KKQ_{25}KK$[32] (peptide sequences listed in Table 1), to explore the effects of N-terminally fused helix-rich domains on cross-β-sheet assembly and aggregation. The influence of the 17-residue N-terminal domain from the huntingtin protein (Htt^{NT}) is compared to that of a designed coiled-coil sequence (ecK)[24] on the kinetics of polyglutamine assembly. Htt^{NT} is known to significantly increase the rate of polyglutamine assembly; however, it is poorly understood how the structural and/or chemical characteristics of this sequence accomplish this increase in rate. It is thought that helix-pairing interactions within the Htt^{NT} domain play a critical role. As a prelude, a comparison is made between the biophysical and structural characteristics of this sequence and that of a well-characterized coiled-coil sequence in preparation for a study of how such sequences influence polyglutamine aggregation. An understanding of the biophysical and structural characteristics of Htt^{NT} provides an opportunity for a deeper molecular interpretation of the role of flanking sequences in modulating polyglutamine aggregation.

Characterization of ecK and Htt^{NT}. Two peptide sequences exploited for this study were derived from our earlier work, involving the design and characterization of a heterotetrameric coiled coil.[24] These peptides include ecK, which contains a total of eight lysine residues distributed in "c" and "e" heptad positions, and ecE, containing glutamates at these same positions. These peptides when prepared individually in solution are essentially disordered, and only upon mixing is a stable four-chain coiled coil formed, held together in part by salt bridges between the lysines and glutamates (Figure 1). Therefore, it appears that the ecK sequence, having disordered characteristics similar to those of Htt^{NT}, would be a good model for comparison as a weakly associating coiled-coil system.

CD spectra of Htt^{NT} and ecK are very similar when measured in the low micromolar range (Figure S2 of the Supporting Information), having features expected for largely unfolded peptides (15 and 16% helix content, respectively[33]), and in the case of Htt^{NT}, representing its likely conformation as an intrinsically disordered domain in the intact huntingtin protein. In both peptides, nonpolar residues are thought to play an important role in driving coiled-coil assembly. The contribution of the hydrophobic effect to protein stability can be approximated by taking advantage of the salting out (or Hofmeister) effect,[34] and this feature is explored in the Supporting Information. To demonstrate the acquisition of helical structure at higher peptide concentrations, titrations were conducted as shown in Figure S1B of the Supporting

dx.doi.org/10.1021/bi500449a | Biochemistry 2014, 53, 6738−6746

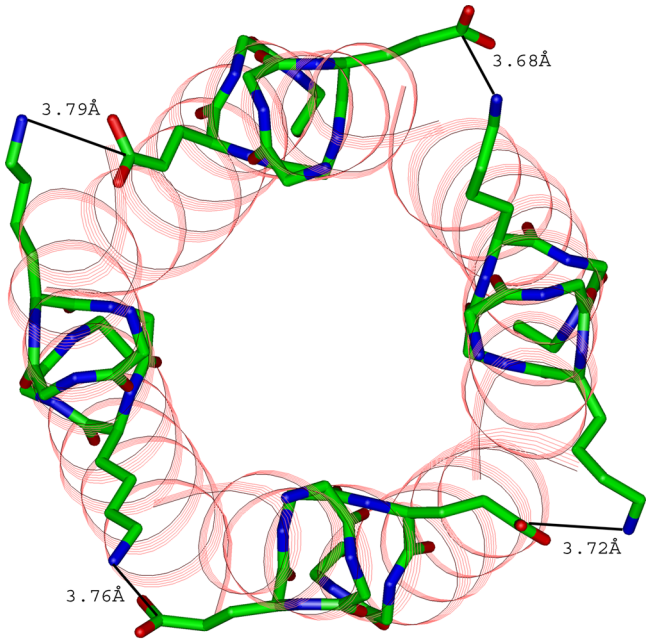

Figure 1. Ribbon and stick model of the ecK/ecE coiled-coil heterotetramer. Stick representations of the lysine and glutamate residues emphasize the ion pair interactions between these residues at the interfaces of the helices. The sequences used to build the model are shown (ecE and ecK). Reproduced from ref 24. Copyright 2009 John Wiley & Sons, Inc.

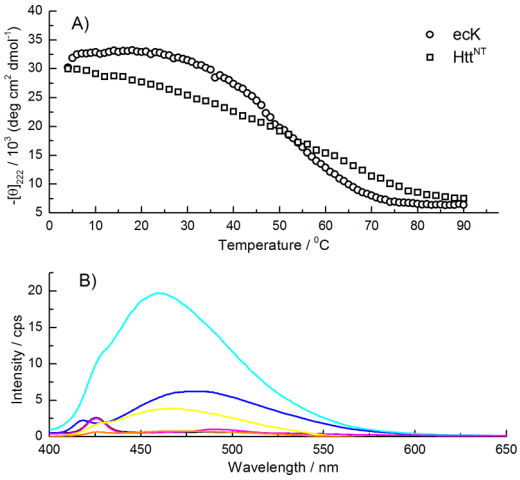

Figure 2. (A) Comparison of helix content as a function of temperature for ecK and Htt^{NT}, as measured by CD. The ecK concentration used was 150 μM in 0.75 M NaCl, and the Htt^{NT} concentration used was 124.5 μM in 1.25 M NaCl. Both were measured in PBS (pH 7.1) at 25 °C. (B) Comparison of ANS binding for ecK (orange) and Htt^{NT} (yellow, with an intensity of ~5 cps) to that of ANS alone (black, overlapped with lysozyme spectrum), 99% EtOH (blue), apomyoglobin (cyan, with an intensity of ~20 cps), and lysozyme (magenta), as measured by fluorescence. All samples were prepared with 1 μM ANS in PBS (pH 7.1) at 25 °C.

Information (see also panels A and C of Figure S2 of the Supporting Information for full CD spectra). Both Htt^{NT} and ecK show fully helical content at peptide concentrations of >50 μM and have similar stability profiles, suggesting that ecK would be a reasonable model for testing the role of coiled-coil stability on polyglutamine aggregation. To further the biophysical analysis, thermal stabilities of the two peptides were measured, again using CD (Figure 2A), revealing a significant difference in the cooperativity of folding. While oligomeric heterogeneity is certainly a hallmark of the behavior of Htt^{NT}, this thermal unfolding behavior is more consistent with an ill-defined hydrophobic core, in which the folded, or collapsed, structure is likely to be dynamic and perhaps possesses molten globule characteristics. It may be that the observed oligomeric heterogeneity is a manifestation of this structural property of the peptide. ANS, a dye that intercalates into dynamic nonpolar cores,[35−37] was used to test the molten globule hypothesis (Figure 2B). There is a significant increase in the fluorescence of ANS upon mixing with Htt^{NT}, similar to the effect seen upon binding of ANS to apomyoglobin, a protein whose molten globule characteristics are well-established. In contrast, ANS shows no fluorescence upon being mixed with ecK, confirming our earlier study showing that this peptide forms a coiled coil with a well-structured core.[24] These differences in biophysical behavior may be of critical importance in interpreting differences in kinetic behavior for the fusion constructs discussed below.

The oligomeric states of these peptides were probed directly using sedimentation velocity experiments. In previous work, it had been shown that the ecK peptide, when mixed with the ecE peptide, forms stable heterotetramers.[24] The ecK peptide by itself is largely monomeric at low micromolar concentrations. At higher concentrations, at which significant oligomerization was expected on the basis of the acquisition of helix content as a function of increasing peptide concentration (as shown in Figure S1B of the Supporting Information), ecK sedimented with an $s_{20,w}$ of 1.10 S, which when coupled to a best fit value of $D_{20,w}$ of 10.61 × 10^{-7} cm^2 s^{-1}, results in a molecular weight close to that expected for a tetramer. The Htt^{NT} peptide showed greater polydispersity, with at least two species, with $s_{20,w}$ values of 1.12 and 1.83 S, which when coupled to the measured $D_{20,w}$ values of 13.10 × 10^{-7} and 5.93 × 10^{-7} cm^2 s^{-1} correspond to molecular weights of tetramer and above. Such nonspecific self-assembly is consistent with molten globule behavior.

Characterization of $KKQ_{25}KK$ and $ecKQ_{25}KK$. Having established basic biophysical characteristics of these peptides, we studied the influence of ecK on polyglutamine aggregation by fusing it to the $KKQ_{25}KK$ sequence (see Table 1). To increase the level of confidence that comparisons could be made with earlier work exploring the aggregation kinetics of $KKQ_{25}KK$ and $Htt^{NT}Q_{25}KK$, peptides containing polyglutamine sequences (Table 1) were subjected to a disaggregation protocol adapted from Wetzel's work,[38] as described in Materials and Methods. Pre- and postcentrifugation aliquots were analyzed by DLS (Figure S3 of the Supporting Information) to assess the efficacy of the disaggregation protocol. The centrifugation step was most essential in providing a highly purified monomeric pool. Final peptide concentrations for the stock solutions ranged between 215 and 230 μM. CD spectra of freshly disaggregated $KKQ_{25}KK$ were taken to demonstrate that the starting material was largely unfolded (Figure S4 of the Supporting Information).

Confirmation of the kinetic findings for $KKQ_{25}KK$ was conducted, as described by Wetzel and colleagues.[32] They showed, using both ThT binding and an HPLC assay,[39] that the $KKQ_{25}KK$ peptide assembles through a high-energy

dx.doi.org/10.1021/bi500449a | Biochemistry 2014, 53, 6738−6746

nucleation intermediate with a critical nucleus size (n^*) involving two chains. Fibrils of this peptide were shown to be rich in β-sheet, similar to other polyglutamine model systems and various amyloid systems. These findings were reproduced using DCVJ, a dye known to have higher sensitivity and greater selectivity for cross-β-sheet fibrils (Figure S5 of the Supporting Information).[29,40] Data were analyzed as previously described[41,42] using a range of $KKQ_{25}KK$ concentrations. Aggregation kinetics were measured as a function of peptide concentration (Figure S5A of the Supporting Information), and the percent monomer was plotted as a function of time (Figure S5B of the Supporting Information), as previously described.[32] The midpoints of each kinetic experiment were used to replot the data with the time parameter plotted as a function of peptide concentration (Figure S5C of the Supporting Information). Finally, the data from Figure S5C of the Supporting Information were then used to generate a log−log plot of the slope as a function of peptide concentration (Figure S5D of the Supporting Information). The data set was then fit with a straight line with a resultant slope of 3.39 ± 0.04, which corresponds to an n^* value of 1.4. The n^* value for $KKQ_{25}KK$ was previously reported to be equal to 2 with a log−log slope variation between 3.86 and 4.31.[32] Such variation in the n^* value is not surprising given the complexity of the disaggregation protocol and slight variations in the disaggregation procedure used here. Additionally, it is possible that the use of different dyes might result in some variation, as well, particularly if the binding of the dye itself might influence the kinetics of aggregation, a problem that has not been addressed adequately in the literature.

The kinetics of aggregation were studied for our $ecKQ_{25}KK$ coiled-coil-polyglutamine hybrid construct to compare our results to both those for $KKQ_{25}KK$ and those for the more recently studied $Htt^{NT}Q_{25}KK$ fusion construct.[12] A kinetic analysis of the aggregation was performed for $ecKQ_{25}KK$ at a variety of concentrations (Figure S6A of the Supporting Information), akin to that reported above for the $KKQ_{25}KK$ peptide. At comparable monomer concentrations (~140 μM), $KKQ_{25}KK$ aggregates with a $t_{1/2}$ equal to 87.5 ± 2.7 h, similar to values seen previously,[32] and can be compared to that observed for $ecKQ_{25}KK$ [238 ± 5 h (Figure 3A)]. Most notably, the ecK fusion construct aggregates at a rate that is much slower than that observed for the $Htt^{NT}Q_{25}KK$ fusion construct, as shown in our own work (see Figure S8 of the Supporting Information; $t_{1/2}$ of 3.2 h when measured at a monomer concentration of 33.7 μM), and that reported previously ($t_{1/2}$ of 25 h when measured at a monomer concentration of ~5 μM).[12] Given the incomplete aggregation isotherms in the time frame of the kinetic measurements, n^* values could not be determined with any level of precision. The features that ecK and Htt^{NT} share in common include being largely monomeric in solution and showing weak helical propensity. Therefore, these properties can be discounted as explanations for our disparate results.

To confirm the presence of β-sheet in the aggregation pathway of the $ecKQ_{25}KK$ peptide, the acquisition of secondary structure was measured using CD as a probe. Figure 4A shows CD spectra collected immediately upon disaggregation, and after being incubated for 7 and 14 days. As expected, the peptide is mostly unfolded at time zero. At day 14, the peptide is largely in a β-sheet conformation, consistent with that inferred from the ThT binding assay. It was interesting to note that on day 7 the peptide shows a decidedly α-helical character,

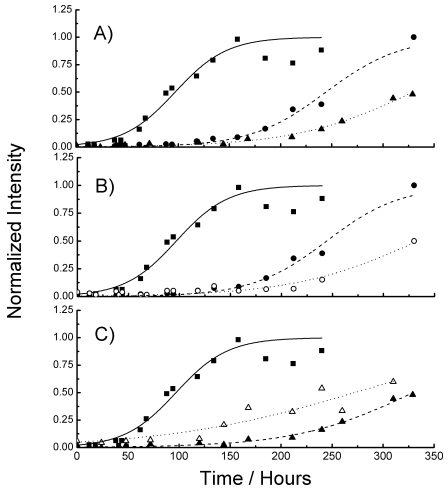

Figure 3. Kinetics of aggregation of peptides used in this study, as monitored by changes in ThT fluorescence intensity. The data are shown fit with a kinetic function as described in Materials and Methods. (A) Aggregation kinetics of $KKQ_{25}KK$ (solid line and filled squares), $ecKQ_{25}KK$ (dashed line and filled circles), and ecK-Ω-$Q_{25}KK$ (dotted line and filled triangles). (B) Kinetics of $ecKQ_{25}KK$ aggregation in the absence (dashed line and filled circles, from panel A) and presence (dotted line and empty circles) of equimolar ecE peptide, as compared to $KKQ_{25}KK$ (solid line and filled squares, from panel B). (C) Kinetics of ecK-Ω-$Q_{25}KK$ aggregation in the absence (dashed line and filled triangles, from panel A) and presence (dotted line and empty triangles) of equimolar ecE peptide, again as compared to $KKQ_{25}KK$ (solid line and filled squares, from panel B). The total monomer peptide concentrations are kept constant at 140 μM, prepared in 30 μM ThT and PBS (pH 7.1) and measured at 25 °C.

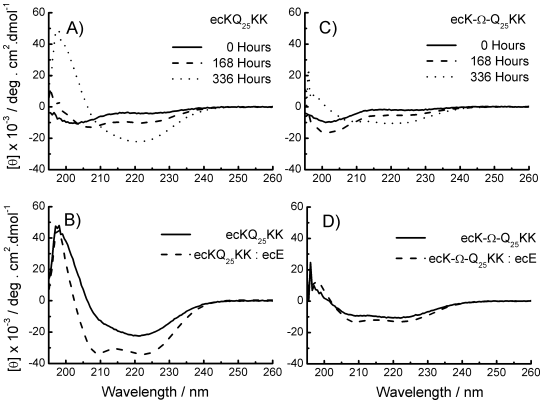

Figure 4. Kinetics of aggregation followed by CD spectra of $ecKQ_{25}KK$ and ecK-Ω-$Q_{25}KK$. (A) CD spectra of $ecKQ_{25}KK$ diluted aggregates at three time points. Mature $ecKQ_{25}KK$ samples in PBS (pH 7.1) were diluted to a total monomer concentration of 20 μM. (B) Comparison of $ecKQ_{25}KK$ with and without ecE on day 14 using a total monomer concentration of 20 μM. (C) Same conditions as in panel A for the CD analysis of ecK-Ω-$Q_{25}KK$. (D) Comparison of ecK-Ω-$Q_{25}KK$ with and without ecE.

suggesting the possibility that an intermediate in the aggregation pathway involves coiled-coil assembly, as proposed previously.[12]

Because ecK alone is highly unstable as a coiled-coil homotetramer, the ecE peptide was added to test the effect of stabilizing the coiled coil on fibril aggregation, which would incorporate interhelix salt bridge interactions. On the basis of a proximity model, it is expected that stabilization would result in

dx.doi.org/10.1021/bi500449a | Biochemistry 2014, 53, 6738−6746

accelerated aggregation due to an increase in the effective concentration of the polyglutamine sequences. The results of the addition of ecE to ecKQ$_{25}$KK in a ThT binding assay are shown in Figure 3B and suggest further inhibition of the kinetics of aggregation to a $t_{1/2}$ projected to be greater than 300 h. It should be noted though that the polyglutamine sequences are being diluted by 2-fold because assembled heterotetramers would now have only two polyglutamine sequences in the proximity of one another, so our results must be interpreted with all due caution. Interestingly, we find that the addition of the ecE peptide results in both the enhanced stability of the coiled coil and the persistence of helix content over time (Figure 4B). Particularly intriguing in the results presented in Figure 4B is the magnitude of the CD signal at 222 nm, with a mean residue ellipticity of approximately −35000 deg cm^2 dmol^{-1}, suggesting that the entire peptide is in a helical conformation, including the polyglutamine domain. A comparison with the results for the ecK-Ω-Q$_{25}$KK:ecE complex (see below) is particularly instructive with respect to the role of helix stabilization in the conformation of polyglutamine.

The aggregation state of ecKQ$_{25}$KK was determined by DLS at a time point at which the helical conformation is present (Figure 4A) and ThT binding is negligible (Figure 3A). Panels A and B of Figure S7 of the Supporting Information show a significant increase in light scattering after 150 h, which when coupled with the CD results suggests that the helical conformation is correlated with limited aggregation. A kinetic analysis, as measured by DLS, also shows that an increase in light scattering temporally precedes binding of the ThT dye, suggesting that aggregation and helix formation help to define a highly populated intermediate prior to the induction of aggregation due to the cross-β-sheet as monitored by ThT (Figure 5A). Helix-induced aggregation preceding cross-β-sheet aggregation has been noted in polyglutamine aggregation studies from other laboratories.[43,44]

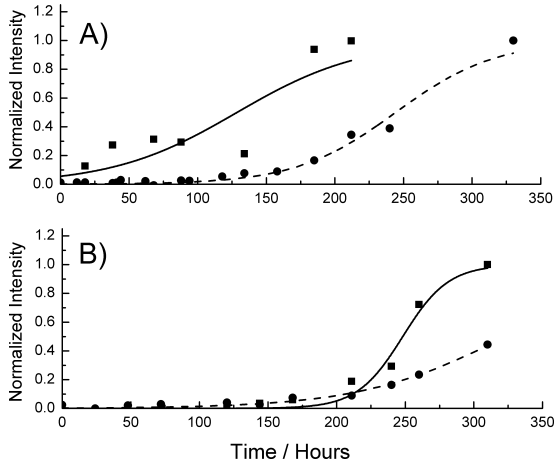

Figure 5. Kinetics of aggregation for (A) ecKQ$_{25}$KK and (B) ecK-Ω-Q$_{25}$KK as monitored by DLS (solid line and squares) and ThT binding (dashed line and circles). The data are shown fit with a kinetic function as described in Materials and Methods. Peptide concentrations are 140 μM. The ThT data are taken from Figure 3 and normalized to emphasize the difference in aggregation kinetics between the two techniques. The normalization for both the ThT binding and DLS data required estimation of the signal for the aggregated species, therefore quantifying the kinetic analysis is not justified.

Characterization ecK-Ω-Q$_{25}$KK and Htt^{NT}-Ω-Q$_{25}$KK. To test the hypothesis that helix propagation into the polyglutamine sequence can increase the rate of aggregation (transformation model), a peptide was designed in which a helix-stopping linker sequence is inserted between the coiled-coil sequence and the polyglutamine sequence [ecK-Ω-Q$_{25}$KK (sequence shown in Table 1)]. The proline and glycine residues in the linker would act to prevent propagation of the helix into the polyglutamine sequence, while the combination of glycines and serines applies established design principles to ensure chain flexibility and solubility.[45] The aggregation kinetics for this peptide were studied at a set of peptide concentrations similar to that reported for ecKQ$_{25}$KK (Figure S6B of the Supporting Information) and compared to that for ecKQ$_{25}$KK and KKQ$_{25}$KK at a single concentration (Figure 3A). A significant inhibition of the rate of aggregation is noted (with a $t_{1/2}$ equal to 315.3 ± 3.0 h for ecK-Ω-Q$_{25}$KK) when compared to that of the peptide without the linker sequence ($t_{1/2}$ equal to 238 ± 5 h).

CD spectra collected for ecK-Ω-Q$_{25}$KK (Figure 4C) at the same time points as those measured for ecKQ$_{25}$KK show minor but interesting differences. On day 7, the peptide, while slightly more helical than at time zero, is still significantly unfolded and is minimally aggregated (Figure S7C,D of the Supporting Information), and on day 14, there has been little maturation to β-sheet, consistent with the lack of ThT binding. Addition of the ecE peptide, while also stabilizing the coiled-coil structure (Figure 4D), results in a mean residue ellipticity of less than −15000 deg cm^2 dmol^{-1}, which suggests that the polyglutamine domain remains largely unfolded, most likely because of the helix-stopping linker preventing propagation of the ecK helix into the polyglutamine sequence. Interestingly, there is little difference in the kinetics of aggregation for ecK-Ω-Q$_{25}$KK in the presence or absence of ecE (Figure 3C), suggesting that isolating the helical conformation to the ecK sequence relieves the influence of coiled-coil stabilization and subsequent propagation into the polyglutamine sequence on cross-β-sheet aggregation as seen for ecKQ$_{25}$KK. What is surprising perhaps is that no inhibition due to polyglutamine dilution in the heterotetramer is observed. Overall, it can be concluded that a comparison of the kinetic results obtained from ecK fusion peptides with and without the linker supports a limited stimulation of kinetic rate in the absence of the helix-stopping sequence that may be correlated with helical transformation of the polyglutamine sequence. The magnitude of this effect, though, is insufficient to provide an explanation for the rapid kinetics of assembly of the Htt^{NT}-Q$_{25}$ fusion construct seen in both in our work and in previous work.[12]

Finally, to complete the test of the transformation model, we compared the kinetics of aggregation of Htt^{NT}Q$_{25}$KK and that of Htt^{NT}-Ω-Q$_{25}$KK (sequences shown in Table 1). Both DLS and ThT assays were conducted (Figure S8 of the Supporting Information) for the two Htt^{NT} peptides. It is noted that our results for Htt^{NT}Q$_{25}$KK are similar to those reported previously, after correcting for concentration effects.[12] Both peptides (with and without the linker) show indistinguishable rapid kinetics of aggregation. These results suggest that helix transformation is not a significant factor in the aggregation kinetics of Htt^{NT} fusions, whereas for the ecK fusions, it does appear that propagation of the helical conformation into the polyglutamine domain might slightly accelerate aggregation.

dx.doi.org/10.1021/bi500449a | Biochemistry 2014, 53, 6738−6746

DISCUSSION

It has been shown previously that a 17-amino acid N-terminal segment from the huntingtin protein (Htt^{NT}) causes a dramatic increase in polyglutamine aggregation rate when compared to that seen with the simple polyglutamine sequence alone.[16] Our goal was to understand what properties of the structure formed by the Htt^{NT} sequence might be responsible for these effects on the aggregation mechanism and kinetics compared to that which is seen with simple polyglutamine peptide model systems. Hence, a comparison of the effects of a well-understood coiled-coil model system to that seen with the Htt^{NT} sequence on polyglutamine aggregation was made, testing the set of hypotheses outlined in the introductory section.

The results show that a peptide that forms a canonical coiled coil (specifically, a tetramer), when fused to a polyglutamine sequence, greatly inhibits the aggregation rate of such a sequence. By exploring a set of sequence variants, we found the results show that this inhibitory affect cannot be ascribed to a straightforward biochemical effect, such as increasing effective concentration, as proposed in the proximity model. Rather, it is likely to be a complex combination of subtle hydrophobic and dynamic effects in the coiled-coil domain itself, as well as the effects of the sequence composition in interactions between this domain and the polyglutamine domain.

It has been shown that the Htt^{NT} domain, which flanks the polyglutamine sequence in the huntingtin protein, forms transient reversible helix-rich tetramers, and that such tetramers further assemble to octamers and higher-order species, either when fused to a polyglutamine sequence[12] or as an independent unit (as demonstrated in our sedimentation velocity study). Our biophysical analysis of the Htt^{NT} sequence suggests that the nonspecific nature of oligomerization may arise from the molten globule-like characteristics of its structure. Such oligomeric heterogeneity has been suggested to be an important influence in the details of the nucleation and subsequent aggregation behavior of these peptides.[21] The ability to access higher-order oligomeric states with Htt^{NT} fusions but not with our ecK fusions suggests that the former oligomers would have a higher local concentration of polyglutamine. At best, our system would have no more than four polyglutamine domains present in the oligomeric structure, whereas those containing the Htt^{NT} fusion may have as many as 12−16 such domains. Thus, the acceleration in kinetics that is observed in the Htt^{NT} model system, relative to our ecK model system, provides some support for the proximity model. However, a critical finding in our results that is inconsistent with the proximity model is that both ecK fusion constructs result in aggregation slower than that of the parent peptide, $KKQ_{25}KK$, which we and others have shown to elongate into fibrils from a nucleation state of a monomer or dimer.[32]

On the basis of suggestions made by Kandel, Hendrickson, and others,[17] it was also intriguing to test how flanking coiled-coil domains might impact aggregation rates based on helical transformation of the polyglutamine domain (transformation model), and our data show that a highly stable coiled coil can indeed rapidly induce an adjacent polyglutamine sequence to become helical. It is not unprecedented for polyglutamine domains to adopt the secondary structure contained within an adjacent amino acid sequence through a propagation mechanism.[14] While the $ecKQ_{25}KK$ construct is 100% helical early in a kinetic profile, it cannot be ascertained whether such a structure is off-pathway or on-pathway in going toward the cross-β-fibril aggregation as observed at a later time. Upon insertion of a helix-stopping linker sequence between the coiled-coil domain and the polyglutamine domain, a slight inhibition of the rate of aggregation is seen. Therefore, assuming an on-pathway mechanism, the helical conformation of the polyglutamine domain may more readily adopt a cross-β-sheet conformation than an intrinsically disordered domain as the starting point, as present in the peptide with the helix-stopping linker. It is formally possible that the introduction of the loop sequence itself might further inhibit the acquisition of a β-strand conformation in the polyglutamine domain and explain the slight inhibition.

In spite of the small difference in aggregation rates that is observed for the two ecK fusions, the transformation model cannot account fully for the large difference in rate that is observed between the rate for Htt^{NT} fused directly to a Q_{25} sequence and that for the ecK-modified Q_{25} constructs. To further support this conclusion, the same helix-stopping sequence was placed in the Htt^{NT}-Q_{25} fusion construct, and experimental analysis revealed no effect on the rate of aggregation upon comparison of the two Htt^{NT}-derived peptides. One last point that can be addressed in this analysis is the disposition of the coiled-coil domain after cross-β-sheet aggregation. In the following paper in this issue (DOI: 10.1021/bi501066q), focusing on details of the morphology of resultant fibrils, the coiled-coil domains appear as irregular pendant structures on a core cross-β-sheet fibril, thus not likely contributing to the overall architecture of these mesoscale structures once they are formed.

Our findings seem most consistent with a domain cross-talk model in offering an explanation for the difference in kinetics between the two model systems. In this model, as described by Pappu and his colleagues,[20] interactions between the Htt^{NT} domain and the polyglutamine domain are critical in determining the aggregation pathway and that the strength of these interactions depends upon both the polyglutamine length and the lack of structural order in both of these domains. It is generally thought that a highly collapsed disordered state may promote nonspecific protein aggregation,[22] and Pappu and his colleagues suggest that such aggregated disordered states, when present in polyglutamine domains, can act to inhibit reorganization into a conformation that can lead productively to the cross-β-sheet fibrillar structure. They propose that the Htt^{NT} domain can attenuate the aggregation of this disordered state by direct intrachain interaction. This interaction depends as well on the degree to which the Htt^{NT} domain is itself behaving as a collapsed and disordered state. Highly charged flanking sequences, lacking in nonpolar residues, cannot readily form collapsed states and thus are less likely to allow domain cross-talk. In the case of the Htt^{NT} sequence, its overall lack of charge and particular distribution of nonpolar side chains would favor domain cross-talk, which can then act to favor a polyglutamine state that is more prone to fibrillar aggregation rather than nonspecific aggregation. This holds particularly for polyglutamine sequences that are ≤25 residues in length.[23] This interpretation is consistent with published data that show that phosphorylation of serine residues at positions 13 and 16 in the Htt^{NT} sequence suppresses huntingtin amyloid accumulation.[46] Our ecK peptide has a net charge of +8 (the net charge on Htt^{NT} is only +1); thus, this offers a ready explanation for why the rate of aggregation is so much slower than that of the Htt^{NT} fusion construct, reiterating the point that highly charged

chains cannot readily form collapsed states or interact with other collapsed domains. This charge effect also likely explains why the kinetics of aggregation is slower than that of the parent peptide, $KKQ_{25}KK$, due to electrostatic repulsive effects. Neither the transformation model nor the proximity model can adequately reconcile this unusually slow assembly process. If the domain cross-talk model is the dominant operating principle, then one would not expect much of a difference in aggregation kinetics in the presence or absence of the helix-stopping linker because there is no effect on the net charge or distribution of nonpolar residues upon introduction of this sequence. This is borne out by the lack of a large difference in the kinetic rates for the two ecK peptide constructs, or in the two Htt^{NT} peptide constructs for that matter.

In summary, while the transformation model can be ruled out as an explanation for the rapid aggregation of polyglutamine domains in the presence of the Htt^{NT} flanking sequence, the proximity model cannot be fully ruled out as having some impact on aggregation rates. However, the data presented here best support a more complex behavior involving domain interactions, or "cross-talk", as proposed by Pappu and others.[19−21,23]

■ ASSOCIATED CONTENT

Supporting Information

CD analysis of the NaCl and peptide concentration dependence for Htt^{NT} and ecK (Figure S1), full CD spectra of the titration experiments shown in Figure S1 (Figure S2), DLS analysis of the disaggregation protocol (Figure S3), structural and kinetic analysis for comparison to previous work on $KKQ_{25}KK$ (Figures S4 and S5), original kinetic traces as measured by ThT binding for $ecKQ_{25}KK$ and ecK-Ω-$Q_{25}KK$ (Figure S6), DLS data for $ecKQ_{25}KK$ and ecK-Ω-$Q_{25}KK$ (Figure S7), and DLS and ThT data for Htt^{NT}-Ω-$Q_{25}KK$ (Figure S8). This material is available free of charge via the Internet at http://pubs.acs.org.

■ AUTHOR INFORMATION

Corresponding Author

*E-mail: rfairman@haverford.edu. Telephone: (610) 896-4205. Fax: (610) 896-4963.

Funding

We gratefully acknowledge funding support from the National Science Foundation (Grant MCB-0516025 to R.F.) and a grant to Haverford College from the Howard Hughes Medical Institute Undergraduate Science Education Program to support undergraduate research.

Notes

The authors declare no competing financial interest.

■ ACKNOWLEDGMENTS

We thank R. Wetzel for advice and training in the disaggregation protocol for the polyglutamine peptides used in this study. We thank R. Pappu for helpful discussions in interpreting our data. We also express our gratitude to K. Johnson for helpful discussions and critical reading of the manuscript. We thank the Department of Biochemistry and Biophysics at the University of Pennsylvania for the use of their MALDI-TOF mass spectrometer.

■ ABBREVIATIONS

ANS, 1-anilinonaphthalene-8-sulfonate; CD, circular dichroism spectropolarimetry; DCVJ, 4-(dicyanovinyl) julolidine; DLS, dynamic light scattering; HFIP, 1,1,1,3,3,3-hexafluoro-2-propanol; MALDI-TOF, matrix-assisted laser desorption ionization time-of-flight; RP-HPLC, reversed phase high-performance liquid chromatography; SV, sedimentation velocity; TFA, trifluoroacetic acid; ThT, thioflavin T.

■ REFERENCES

(1) Wetzel, R. (2012) Physical chemistry of polyglutamine: Intriguing tales of a monotonous sequence. *J. Mol. Biol. 421*, 466−490.

(2) Dobson, C. M. (2001) The structural basis of protein folding and its links with human disease. *Philos. Trans. R. Soc., B 356*, 133−145.

(3) Sikorski, P., and Atkins, E. (2005) New model for crystalline polyglutamine assemblies and their connection with amyloid fibrils. *Biomacromolecules 6*, 425−432.

(4) Perutz, M. F., Johnson, T., Suzuki, M., and Finch, J. T. (1994) Glutamine repeats as polar zippers: Their possible role in inherited neurodegenerative diseases. *Proc. Natl. Acad. Sci. U.S.A. 91*, 5355−5358.

(5) Kirkitadze, M. D., Condron, M. M., and Teplow, D. B. (2001) Identification and characterization of key kinetic intermediates in amyloid β-protein fibrillogenesis. *J. Mol. Biol. 312*, 1103−1119.

(6) Williamson, J. A., Loria, J. P., and Miranker, A. D. (2009) Helix stabilization precedes aqueous and bilayer-catalyzed fiber formation in islet amyloid polypeptide. *J. Mol. Biol. 393*, 383−396.

(7) Wiltzius, J. J., Sievers, S. A., Sawaya, M. R., and Eisenberg, D. (2009) Atomic structures of IAPP (amylin) fusions suggest a mechanism for fibrillation and the role of insulin in the process. *Protein Sci. 18*, 1521−1530.

(8) Abedini, A., and Raleigh, D. P. (2009) A critical assessment of the role of helical intermediates in amyloid formation by natively unfolded proteins and polypeptides. *Protein Eng., Des. Sel. 22*, 453−459.

(9) Abedini, A., and Raleigh, D. P. (2009) A role for helical intermediates in amyloid formation by natively unfolded polypeptides? *Phys. Biol. 6*, 015005.

(10) Goldsbury, C., Goldie, K., Pellaud, J., Seelig, J., Frey, P., Muller, S. A., Kistler, J., Cooper, G. J., and Aebi, U. (2000) Amyloid fibril formation from full-length and fragments of amylin. *J. Struct. Biol. 130*, 352−362.

(11) Mishra, R., Jayaraman, M., Roland, B. P., Landrum, E., Fullam, T., Kodali, R., Thakur, A. K., Arduini, I., and Wetzel, R. (2012) Inhibiting the nucleation of amyloid structure in a huntingtin fragment by targeting α-helix-rich oligomeric intermediates. *J. Mol. Biol. 415*, 900−917.

(12) Jayaraman, M., Kodali, R., Sahoo, B., Thakur, A. K., Mayasundari, A., Mishra, R., Peterson, C. B., and Wetzel, R. (2012) Slow amyloid nucleation via α-helix-rich oligomeric intermediates in short polyglutamine-containing huntingtin fragments. *J. Mol. Biol. 415*, 881−899.

(13) Kelley, N. W., Huang, X., Tam, S., Spiess, C., Frydman, J., and Pande, V. S. (2009) The predicted structure of the headpiece of the Huntingtin protein and its implications on Huntingtin aggregation. *J. Mol. Biol. 388*, 919−927.

(14) Kim, M. W., Chelliah, Y., Kim, S. W., Otwinowski, Z., and Bezprozvanny, I. (2009) Secondary structure of Huntingtin amino-terminal region. *Structure 17*, 1205−1212.

(15) Jayaraman, M., Mishra, R., Kodali, R., Thakur, A. K., Koharudin, L. M., Gronenborn, A. M., and Wetzel, R. (2012) Kinetically competing huntingtin aggregation pathways control amyloid polymorphism and properties. *Biochemistry 51*, 2706−2716.

(16) Thakur, A. K., Jayaraman, M., Mishra, R., Thakur, M., Chellgren, V. M., Byeon, I. J., Anjum, D. H., Kodali, R., Creamer, T. P., Conway, J. F., Gronenborn, A. M., and Wetzel, R. (2009) Polyglutamine disruption of the huntingtin exon 1 N terminus triggers a complex aggregation mechanism. *Nat. Struct. Mol. Biol. 16*, 380−389.

(17) Fiumara, F., Fioriti, L., Kandel, E. R., and Hendrickson, W. A. (2010) Essential role of coiled coils for aggregation and activity of Q/N-rich prions and PolyQ proteins. *Cell 143*, 1121−1135.
(18) Sivanandam, V. N., Jayaraman, M., Hoop, C. L., Kodali, R., Wetzel, R., and van der Wel, P. C. A. (2011) The Aggregation-Enhancing Huntingtin N-Terminus Is Helical in Amyloid Fibrils. *J. Am. Chem. Soc. 133*, 4558−4566.
(19) Crick, S. L., Ruff, K. M., Garai, K., Frieden, C., and Pappu, R. V. (2013) Unmasking the roles of N- and C-terminal flanking sequences from exon 1 of huntingtin as modulators of polyglutamine aggregation. *Proc. Natl. Acad. Sci. U.S.A. 110*, 20075−20080.
(20) Mao, A. H., Crick, S. L., Vitalis, A., Chicoine, C. L., and Pappu, R. V. (2010) Net charge per residue modulates conformational ensembles of intrinsically disordered proteins. *Proc. Natl. Acad. Sci. U.S.A. 107*, 8183−8188.
(21) Vitalis, A., and Pappu, R. V. (2011) Assessing the contribution of heterogeneous distributions of oligomers to aggregation mechanisms of polyglutamine peptides. *Biophys. Chem. 159*, 14−23.
(22) Uversky, V. N., and Fink, A. L. (2004) Conformational constraints for amyloid fibrillation: The importance of being unfolded. *Biochim. Biophys. Acta 1698*, 131−153.
(23) Williamson, T. E., Vitalis, A., Crick, S. L., and Pappu, R. V. (2010) Modulation of polyglutamine conformations and dimer formation by the N-terminus of huntingtin. *J. Mol. Biol. 396*, 1295−1309.
(24) Root, B. C., Pellegrino, L. D., Crawford, E. D., Kokona, B., and Fairman, R. (2009) Design of a heterotetrameric coiled coil. *Protein Sci. 18*, 329−336.
(25) Crestfield, A. M., Moore, S., and Stein, W. H. (1963) The preparation and enzymatic hydrolysis of reduced and S-carboxymethylated proteins. *J. Biol. Chem. 238*, 622−627.
(26) Rosen, H. (1957) A modified ninhydrin colorimetric analysis for amino acids. *Arch. Biochem. Biophys. 67*, 10−15.
(27) Pace, C. N., Vajdos, F., Fee, L., Grimsley, G., and Gray, T. (1995) How to measure and predict the molar absorption coefficient of a protein. *Protein Sci. 4*, 2411−2423.
(28) Wall, J., Schell, M., Murphy, C., Hrncic, R., Stevens, F. J., and Solomon, A. (1999) Thermodynamic instability of human lambda 6 light chains: Correlation with fibrillogenicity. *Biochemistry 38*, 14101−14108.
(29) Mok, Y. F., Ryan, T. M., Yang, S., Hatters, D. M., Howlett, G. J., and Griffin, M. D. (2011) Sedimentation velocity analysis of amyloid oligomers and fibrils using fluorescence detection. *Methods 54*, 67−75.
(30) Roy, S., Ratnaswamy, G., Boice, J. A., Fairman, R., McLendon, G., and Hecht, M. H. (1997) A protein designed by binary patterning of polar and nonpolar amino acids displays native-like properties. *J. Am. Chem. Soc. 119*, 5302−5306.
(31) Schuck, P., and Zhao, H. (2011) Editorial for the special issue of methods "Modern Analytical Ultracentrifugation". *Methods*, 1−3.
(32) Kar, K., Jayaraman, M., Sahoo, B., Kodali, R., and Wetzel, R. (2011) Critical nucleus size for disease-related polyglutamine aggregation is repeat-length dependent. *Nat. Struct. Mol. Biol. 18*, 328−336.
(33) Rohl, C. A., and Baldwin, R. L. (1998) Deciphering rules of helix stability in peptides. *Methods Enzymol. 295*, 1−26.
(34) Baldwin, R. L. (1996) How Hofmeister ion interactions affect protein stability. *Biophys. J. 71*, 2056−2063.
(35) Semisotnov, G. V., Rodionova, N. A., Razgulyaev, O. I., Uversky, V. N., Gripas, A. F., and Gilmanshin, R. I. (1991) Study of the "molten globule" intermediate state in protein folding by a hydrophobic fluorescent probe. *Biopolymers 31*, 119−128.
(36) Mulqueen, P. M., and Kronman, M. J. (1982) Binding of naphthalene dyes to the N and A conformers of bovine α-lactalbumin. *Arch. Biochem. Biophys. 215*, 28−39.
(37) Goto, Y., and Fink, A. L. (1989) Conformational states of β-lactamase: Molten-globule states at acidic and alkaline pH with high salt. *Biochemistry 28*, 945−952.
(38) Chen, S., and Wetzel, R. (2001) Solubilization and disaggregation of polyglutamine peptides. *Protein Sci. 10*, 887−891.
(39) O'Nuallain, B., Thakur, A. K., Williams, A. D., Bhattacharyya, A. M., Chen, S., Thiagarajan, G., and Wetzel, R. (2006) Kinetics and thermodynamics of amyloid assembly using a high-performance liquid chromatography-based sedimentation assay. *Methods Enzymol. 413*, 34−74.
(40) Bertoncini, C. W., and Celej, M. S. (2011) Small molecule fluorescent probes for the detection of amyloid self-assembly in vitro and in vivo. *Curr. Protein Pept. Sci. 12*, 205−220.
(41) Chen, S., Berthelier, V., Hamilton, J. B., O'Nuallain, B., and Wetzel, R. (2002) Amyloid-like features of polyglutamine aggregates and their assembly kinetics. *Biochemistry 41*, 7391−7399.
(42) Chen, S., Berthelier, V., Yang, W., and Wetzel, R. (2001) Polyglutamine aggregation behavior in vitro supports a recruitment mechanism of cytotoxicity. *J. Mol. Biol. 311*, 173−182.
(43) Jayaraman, M., Thakur, A. K., Kar, K., Kodali, R., and Wetzel, R. (2011) Assays for studying nucleated aggregation of polyglutamine proteins. *Methods 53*, 246−254.
(44) Legleiter, J., Mitchell, E., Lotz, G. P., Sapp, E., Ng, C., DiFiglia, M., Thompson, L. M., and Muchowski, P. J. (2010) Mutant huntingtin fragments form oligomers in a polyglutamine length-dependent manner in vitro and in vivo. *J. Biol. Chem. 285*, 14777−14790.
(45) Huston, J. S., Levinson, D., Mudgett-Hunter, M., Tai, M. S., Novotny, J., Margolies, M. N., Ridge, R. J., Bruccoleri, R. E., Haber, E., Crea, R., et al. (1988) Protein engineering of antibody binding sites: Recovery of specific activity in an anti-digoxin single-chain Fv analogue produced in *Escherichia coli*. *Proc. Natl. Acad. Sci. U.S.A. 85*, 5879−5883.
(46) Mishra, R., Hoop, C. L., Kodali, R., Sahoo, B., van der Wel, P. C., and Wetzel, R. (2012) Serine phosphorylation suppresses huntingtin amyloid accumulation by altering protein aggregation properties. *J. Mol. Biol. 424*, 1−14.